Diffusion of Fe atoms on W surfaces and Fe/W films and along surface steps

D. Spišák* and J. Hafner

Institut für Materialphysik and Center for Computational Materials Science, Universität Wien, Sensengasse 8, A-1090 Wien, Austria
(Received 26 May 2004; published 18 November 2004)

The diffusion of Fe atoms on clean W(100) and W(110) surfaces and along surface steps, and the diffusion of Fe adatoms and vacancies on Fe/W(100) and Fe/W(110) films has been investigated using *ab initio* DFT methods. Our results demonstrate that even a single Fe adatom on the W(100) surface induces locally a partial dereconstruction of the surface, leading to an activation energy for hopping diffusion of 1.2 eV which is lower on the reconstructed than on the ideal surface. On W(110) diffusion occurs by elementary jumps along close-packed directions, the calculated activation energies of 0.7 eV are in quantitative agreement with experimental estimates. Exchange diffusion of Fe is unfavorable on both surfaces. The investigations of adatom diffusion on 1-ML Fe films reveal a delicate interplay between structural and magnetic effects. For nonmagnetic Fe/W(100) films, at low coverages (below 0.4 ML) adatoms do not propagate the pseudomorphic structure, but occupy bridge instead of hollow sites. The site preference switches to the hollow at higher coverages. Correspondingly, the potential energy surface is rather smooth, leading to low activation energies for hopping diffusion of 0.4 and 0.5 eV for jumps to nearest- and next-nearest-neighbor sites, respectively. Exchange diffusion requires a larger activation energy of 0.7 eV. Antiferromagnetic ordering of the film completely changes the picture. The magnetic interactions around the adsorbate are necessarily frustrated, the adatom induces the formation of a ferromagnetic defect. As a consequence of the frustration, the potential energy is even flatter than for the nonmagnetic case with an activation energy of only 0.3 eV, leading to the prediction of faster diffusion below the Néel temperature of the film. Fe adatoms on Fe/W(110) induce a local transition from a pseudomorphic to a close-packed arrangement, the adatom is incorporated in the film forming a Fe-Fe dumbbell occupying a lattice site. Our studies are completed by the investigation of vacancy diffusion in Fe/W films and adatom diffusion along step edges. Vacancy diffusion requires a higher activation energy than adatom hopping, in particular in Fe/W(100) films. Diffusion along steps has been studied on a vicinal (110) surface with ⟨100⟩-type steps. The minimal activation energy is with 1.3 eV considerably higher than for diffusion on the terraces. Decoration of the steps with a row of Fe atoms lowers all activation energies, so that diffusion rates on terraces and along Fe-decorated steps are comparable. The implication of our results on the kinetics of film growth are discussed.

I. INTRODUCTION

Scarcely any other metal surface has been studied as intensively as W(100). Since it has been discovered that the clean W(100) surface undergoes a reconstruction from a high-temperature (1×1) to a low-temperature $c(2 \times 2)$ structure[1–3] many experimental and theoretical studies have been devoted to the understanding of the driving force for this surface reconstruction. Because the reconstructed surface can be described as the frozen-in surface phonon mode M_5 with the wave vector $q = \pi/a(110)$ (Ref. 3), a surface charge-density-wave (CDW) mechanism has been invoked to account for the structural transition.[4] However, there seems to be no surface state or resonance around the Fermi level[5,6] along the ΓM symmetry line. More recent angle-resolved photoemission experiments[7] found that a gap of about 0.6 eV opens upon reconstruction, favoring a CDW-like mechanism. Based on first principles calculations of the band structure a local-bonding mechanism has been proposed to be responsible for the surface instability of W(100).[6,8,9] Here it is expected that the energy gain associated with the formation of shorter, tighter bonds between surface atoms along ⟨110⟩ directions outweighs the energy loss due to a displacement of surface atoms out of their ideal bcc positions. In this regard,

it is worthwhile mentioning that the W(100) reconstruction is not restricted to the topmost layer, but it involves displacements in at least two subsurface layers.[9–11] The local-bonding picture suggests that the very origin of the surface reconstruction could be sought in a relief of the surface stress. The surface stress has been recognized as the driving force for the surface reconstruction in late $4d$ and $5d$ transition metals.[12] This point will be one of the subjects discussed in the present paper.

High surface energy in combination with a high melting point makes tungsten a surface frequently used for the growth of high-quality thin films. In this respect, numerous investigations have been devoted to the study of thin Fe films on a W(100) substrate,[13–16] on a W(110) substrate,[17–32] as well as on stepped W substrates.[33–36] These systems have attracted considerable attention as low-dimensional magnetic structures. In one monolayer (ML) thick Fe/W(100) films no sign of ferromagnetic order has been detected, neither by spin-polarized low-energy electron diffraction[14] nor by magneto-optic Kerr effect (MOKE) measurements.[15,16] Above 1-ML coverage the Curie temperature rises linearly with the film thickness. Fe/W(100) film growth falls in one of three categories: (i) At room temperature lateral diffusion is restricted, therefore small islands are observed and the film

roughness increases with the film thickness.[16] (ii) At high temperatures over 800 K the first two layers grow epitaxially, further deposited material forms three-dimensional islands, which are fully relaxed.[13,14,16] (iii) At intermediate temperatures (400–500 K) layer-by-layer growth is observed up to 4 ML thickness, in the fifth layer dislocation lines are spontaneously formed with an average separation of nine atomic rows along the $\langle 100 \rangle$ direction.[16]

As with Fe/W(100) films, Fe films on W(110) are also subject to a large tensile strain, i.e., they prefer a smaller in-plane lattice constant and higher atomic density. Because a (110) plane is a glide plane in bcc crystals, strain relief is operative already in films with a thickness between 1 and 2 ML (Ref. 17). As a consequence of the changed morphology the magnetic properties reveal a pronounced variation on going from 1 to 2 ML thick films. A zero temperature magnetic moment of $m = 2.53 \pm 0.12 \mu_B$ in Fe/W(110) adlayers has been determined by a combination of conversion-electron Mössbauer spectroscopy measuring the temperature-dependent magnetic hyperfine fields with torsion oscillation magnetometry providing the absolute size of magnetic moments.[18] At a coverage of about 1.4 ML an apparent loss of ferromagnetic order has been reported and ascribed to an antiferromagnetic coupling between islands.[24] Later on, this peculiar behavior has been explained in terms of extremely enhanced coercivity at this coverage.[25] By means of STM analysis Bethge et al.[26] showed that in 3-ML films a partial relaxation of the misfit strain along one direction occurs, whereas 4-ML films exhibit a two-dimensional periodic dislocation network. Recently, 13-ML films have been studied by surface x-ray diffraction and a rather complex, laterally and vertically modulated structure has been found with an approximate coincidence of 37 Fe atoms with 34 W atoms.[27]

One-dimensional phenomena have been explored in Fe stripes on stepped W(110) surfaces. A precondition for the growth of smooth stripes are elevated temperatures. Elmers et al.[34] found ferromagnetic order in stripes prepared at 660 K with a nominal coverage of more than 0.05 ML. At 300 K the migration of atoms is hindered and hence films consist of islands with ragged edges. They become ferromagnetic just above the percolation threshold of 0.6 ML. Geometry and magnetic properties of the stripes depend on the step orientation—continuous stripes are formed along the [100] azimuth, whereas the [110]-oriented stripes are composed of triangular islands.[35]

The film structure is governed not only by thermodynamic principles, but also by the kinetics of surface mass transport. To date, diffusion of Fe on tungsten has not been studied as intensively as the static film properties. From their analysis of work function changes, Nahm and Gomer[21] concluded that the activation energy barrier in 0.1-ML Fe/W(110) films amounts to 0.6 eV. From spreading experiments,[36] in which the evolution of the concentration profile around an evaporated circular Fe dot on W(110) was recorded, it has been concluded that in contrast to some other systems, Fe diffusion along step edges is not very different from that on tungsten terraces. Further, the activation energy barrier for Fe diffusion on 1-ML Fe/W(110) films has been estimated at $\Delta E = 1.2$ eV. As to the Fe/W(100) system, we are unaware of any studies of surface diffusion.

The main objective of this paper is the determination of the equilibrium structure and magnetic properties of ultrathin Fe films on W surfaces, further our aim is to establish the prevailing diffusion mechanism on clean and Fe-covered W surfaces. Our approach relies on local-density functional theory. The key details of the first-principles calculations are specified in Sec. II. In Sec. III we compare our results for reconstructed W(100) and relaxed W(110) surfaces with previous calculations and discuss the correlation between reconstruction, surface energy and surface stress. Section IV contains the results on equilibrium structure and magnetic ordering in 1-ML and 2-ML Fe films. Section V is devoted to the investigation of various hopping and exchange diffusion processes on both flat and vicinal surfaces. Finally, in Sec. VI we will summarize our results and draw some conclusions.

II. COMPUTATIONAL DETAILS

Our calculations were carried out within local-density functional theory using the Vienna Ab-initio Simulation Package[40] (VASP). The electron-ion interaction was described by projector augmented wave potentials.[41,42] We used the local exchange-correlation functional parametrized according to Perdew and Zunger[43] with added nonlocal corrections in the form of the generalised gradient approximation (GGA) proposed by Perdew et al.[44] The GGA value for the tungsten lattice constant of $a_W = 3.181$ Å is moderately larger than the measured value of 3.165 Å (Ref. 45), whereas without GGA corrections a much too small lattice constant of 3.133 Å is found. The inclusion of semicore $5p$ states gives a lattice constant of 3.188 Å. Tungsten has an extremely high bulk modulus,[46] $B = 314$ GPa. We obtained $B = 282$ GPa without the $5p$ semicore states and $B = 278$ GPa when these states are taken into account. Because the inclusion of the $5p$ states into the valence basis set does not substantially modify the cohesive properties, we have not considered them in the following.

The plane-wave basis set contained components with energies up to 280 eV, ensuring a good convergence of total energies. The set of k points was adapted to the size of the computational cell. For large models with more than one hundred atoms the Brillouin zone was sampled at Γ point only, for smaller models a Monkhorst-Pack mesh[47] of k points was used, which varied from calculation to calculation. For example, a 1-ML Fe film on W(110) with a $c(2 \times 2)$ surface unit cell was modeled by six substrate layers, one Fe layer and an 13.8 Å thick vacuum region, and 70 irreducible k points were used. The geometric relaxation was done with a quasi-Newton algorithm using the exact Hellmann-Feynman interatomic forces.

The values of the activation energy barriers were typically found by comparing initial and transition state. If the symmetry of the transition state was lower, the energy barriers were calculated using the nudged elastic band method[48] with three images of the system forming a discretization of the path between the fixed end points. Because these calculations require rather extended computational models in order to reduce adatom-adatom interactions, one k point was used in

TABLE I. The calculated lateral displacements (s) and vertical interlayer relaxations (δ) of the surface and two subsurface atoms in W(110) and W(100). For W(100) surface the energy gain upon reconstruction ΔE_r is listed and the values obtained in the present work are compared with other theoretical (Refs. 9 and 11) and experimental (Ref. 10) results.

	W(110)	W(100)	W(100)[a]	Ref. 9	Ref. 11	Ref. 10
s_1 (Å)	0.0	0.27	0.26	0.27	0.22	0.24
s_2 (Å)	0.0	0.04	0.04	0.05	0.05	0.05
s_3 (Å)	0.0	0.01	0.01	0.02		
δ_{12} (%)	−4.7	−7.8	−6.5	−6.0	−4.0	−4.0
δ_{23} (%)	0.2	0.5	0.7	0.5		
δ_{34} (%)	−0.6	−1.1	−0.5			
ΔE_r (meV)		−60	−52			−60

[a]The 5p states treated as the semicore states.

evaluation of sums over the Brillouin zone as a compromise between accuracy and efficiency. This introduces a numerical error of ±0.1 eV in the energy barrier values. In this error estimation we compared the energy barrier obtained using 1 and 4 k points. The previous *ab initio* study of diffusion of Ni adatoms on Ni(100) surfaces[49] has shown that the energy barriers, especially the exchange diffusion energy barriers, converge slowly with the lateral size of the models. We have used sufficiently extended models with (4×4) and (4×3) surface cells for studying adatom and vacancy migration on W(100) and W(110), respectively. Despite quite a large error bar, the dominant diffusion mechanism for each particular system can be determined without doubt as will become apparent below.

III. CLEAN (100) AND (110) TUNGSTEN SURFACES

Because W(100) and W(110) surfaces have been chosen as templates for our investigations of diffusion of Fe adatoms and the growth of ultrathin Fe films, we present first a struc-

tural characterisation of these surfaces in a clean, adsorbate-free state. The W(100) surface has been the subject of numerous studies focusing mainly on understanding its $c(2 \times 2)$ surface reconstruction. Several independent theoretical results for this surface published earlier[9,11] (which considered multilayer relaxation) are used for comparison with our findings. To determine the stable ground-state structure, we have tried various displacement patterns either along the $\langle 100 \rangle$ or the $\langle 110 \rangle$ direction. We used 12-ML thick slabs with two atoms in each layer. The atoms in the first four layers on both sides of the slab were free to relax in any direction, except the lateral coordinates of surface atoms which were constrained to desired positions. The (1×1) W(100) surface is unstable as observed in experiment. The calculated relaxation and reconstruction parameters are given in Table I. The table is completed by Fig. 1 showing the evolution of the total energy and interlayer distances with increasing lateral shifts. In good agreement with experimental data and previous calculations we find a displacement of ±0.27 Å parallel to the $\langle 110 \rangle$ direction in the surface layer and strongly damped displacements in two next layers. As can be seen from Fig. 1, the inward relaxation of the surface layer continuously decreases through the reconstruction as a result of a vanishing registry with the rigid underlying lattice. Table I contains also the results of a structural optimisation in which the 5p states of tungsten were treated as semicore states. To be consistent we have also used the corresponding bulk lattice constant $a_W = 3.188$ Å, calculated with relaxed 5p semicore states in evaluation of relative changes. It turns out that there are no significant changes in the optimized structural parameters, and the energy gain upon reconstruction is reduced from −60 to −52 meV. This underlines the fact that our choice of treating the 5p states as core states in the rest of the study is fully adequate for obtaining reliable structural data and that the calculated energy differences can be considered as accurate within 15%.

To gain a deeper insight into the energetics of the W(100) surface instability we have evaluated the surface energy and
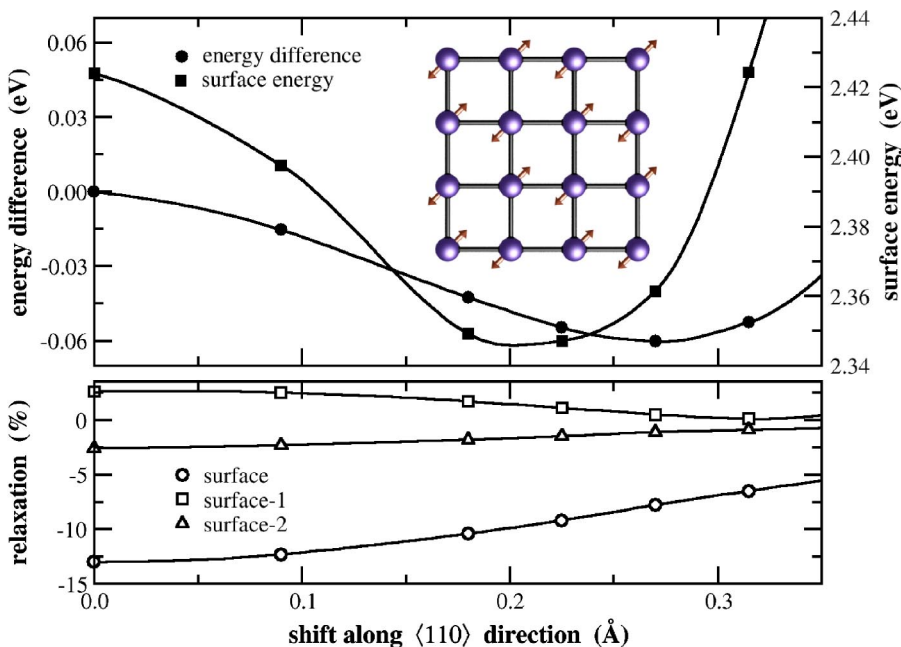

FIG. 1. (Color online) Top panel: total energy against a lateral shift in the surface plane of W(100) relative to the unreconstructed surface (the left scale) and surface energy (the right scale). Both energies are given per surface atom. The inset illustrates the atomic displacements leading to a reconstructed surface. Bottom panel: change of vertical interlayer distances for the three topmost layers upon reconstruction.

the surface stress. The surface energy σ was calculated according to the formula[38]

$$\sigma = \lim_{L \to \infty} \frac{1}{4}\left[E_L - \frac{L}{2}(E_L - E_{L-2}) \right], \quad (1)$$

where E_L means the total energy of a slab with L layers ($L = 12$ in our case) and the factor $1/4$ accounts for two surfaces and two atoms per layer. Equation (1) has the virtue of numerical stability and rapid convergence with slab thickness. The total surface stress τ is related to the variation of the surface energy via

$$\tau_{ij} = \delta_{ij}\sigma + \frac{\partial \sigma}{\partial \epsilon_{ij}}. \quad (2)$$

We estimated the surface energy derivative with respect to the strain ϵ by varying the in-plane lattice constant by ± 0.3 and $\pm 0.6\%$ equally in both lateral directions and then divided the resultant value by two. For a relaxed but unreconstructed W(100) surface a value of $\sigma = 2.42$ eV/atom was obtained. The surface energy is reduced in the course of the reconstruction to 2.35 eV/atom. As seen from Fig. 1, the correlation between the variation of the total energy and the surface energy is not perfect. The minimum in the surface energy is reached for a displacement of nearly 0.2 Å, well before the reconstruction is terminated. This fact forbids an unambiguous identification of the driving force for the reconstruction with the relaxation of the surface energy. This conclusion is reinforced further by analysis of the surface stress. The relaxed W(100) surface is subject to a tensile stress $\tau = 5.06$ eV/atom. As a simple criterion estimating the tendency to reconstruct is the dimensionless ratio[12]

$$\alpha = \frac{1}{aE_c}\frac{\partial \sigma}{\partial \epsilon} = \frac{\tau - \sigma}{aE_c}, \quad (3)$$

between the surface energy derivative $\tau - \sigma$, and the cohesive energy E_c, multiplied with the lattice constant a. The Ir(100), Pt(100), and Au(100) surfaces which reconstruct have $\alpha \geq 0.2$, whereas for W(100) we get merely $\alpha \approx 0.14$.

We evaluated also the surface stress in the reconstructed state. Against expectations the total surface stress *increases* to $\tau = 7.04$ eV/atom. Therefore we arrive at the conclusion that the stabilization of the $c(2 \times 2)$ surface periodicity cannot be attributed to a surface stress relief mechanism, so that a previously discussed local-bonding model[6,8,9] seems more appropriate for this particular system. In fact, the density of states of the reconstructed model (not shown) differs from that of the relaxed model just in a quite narrow energy range between -1 and 1 eV around the Fermi level. The marked spike closely below the Fermi level in the unreconstructed state as well as the density of states at the Fermi level are almost halved in the reconstructed state, favoring reconstruction. Closer inspection reveals that all d orbitals contribute to this feature and it cannot be attributed to some limited part of the Brillouin zone, ruling out a CDW interpretation.

For a W(110) surface lateral displacements do not lead to any energy reduction, demonstrating that this surface relaxes vertically, but does not reconstruct. The vertical relaxations are listed in Table I. These values correlate fairly well with a

TABLE II. The calculated changes of interlayer distances δ with respect to the interlayer distance $d_0^{[100]} = 1.59$ Å or $d_0^{[110]} = 2.25$ Å in bcc tungsten, magnetic moments m, and the energies ΔE_m relative to the ground-state configuration for 1-ML Fe films on W(100) and W(110) substrates. Ferromagnetic (FM), two distinct antiferromagnetic [AF1$=c(2 \times 2)$, AF2$=(2 \times 1)$], and nonmagnetic (NM) solutions have been considered.

	δ_{12} (%)	δ_{23} (%)	m (μ_B)	ΔE_m (meV)
1Fe/W(100)-FM	−29.6	2.8	1.27	116
1Fe/W(100)-AF1	−20.4	0.0	±2.43	0
1Fe/W(100)-AF2	−26.0	2.3	±2.06	54
1Fe/W(100)-NM	−33.2	3.2	0.00	155
1Fe/W(110)-FM	−14.7	−0.1	2.41	0
1Fe/W(110)-AF1	−16.4	0.6	±2.31	137
1Fe/W(110)-AF2	−13.9	−0.1	±2.54	56
1Fe/W(110)-NM	−19.8	0.6	0.0	423

contraction by -3.1% in the top layer and negligible variations of the subsurface interlayer spacings as detected by low-energy electron diffraction (LEED) technique.[37] In general one expects that more open metallic surfaces undergo stronger relaxations. We have found this trend in tungsten too, however, the contraction of the unreconstructed W(100) surface layer of $\delta_{12}^{(100)} = -13.0\%$ is very large in comparison to the $\delta_{12}^{(110)} = -4.7\%$ of the W(110) surface. On the reconstructed W(100) surface the contraction decreases to $\delta_{12}^{(100)} = -7.8\%$, so that the ratio $\delta_{12}^{(100)}/\delta_{12}^{(110)}$ falls in the range common to other bcc metallic surfaces.

IV. THIN Fe/W(100) AND Fe/W(110) FILMS

Having characterised the uncovered W(100) and W(110) surfaces, we turn to a description of one and two monolayer thick iron films grown on these surfaces. For these films until now a ferromagnetic (FM) order has been expected *a priori*. This assumption is indeed justified in the case of Fe/W(110) films, whereas for Fe/W(100) films an antiferromagnetic (AF) order is possible, as follows from Table II. In an Fe monolayer on W(100) a $c(2 \times 2)$ AF alignment, in which each atom is surrounded by atoms carrying an opposite magnetic moment, is by far the most stable solution. The antiferromagnetic moments in the stable phase are nearly twice as large as the moments in the FM phase, the FM film relaxes inward by nearly -30%, while the relaxation is only about -20% in the AF phase. By comparing the density of states of the $c(2 \times 2)$ AF and FM configurations, as displayed in Fig. 2, in addition to the higher density of states at the Fermi level found in the FM film, the second reason for the stability of the AF solution is the enhanced exchange splitting between majority and minority $d_{t_{2g}}$ states pushing the center of the gravity of these states towards higher binding energies. We have verified that a free-standing Fe(100) monolayer in the same atomic arrangement is ferromagnetic and a $c(2 \times 2)$ AF solution has an energy higher by 146 meV/atom, so that the
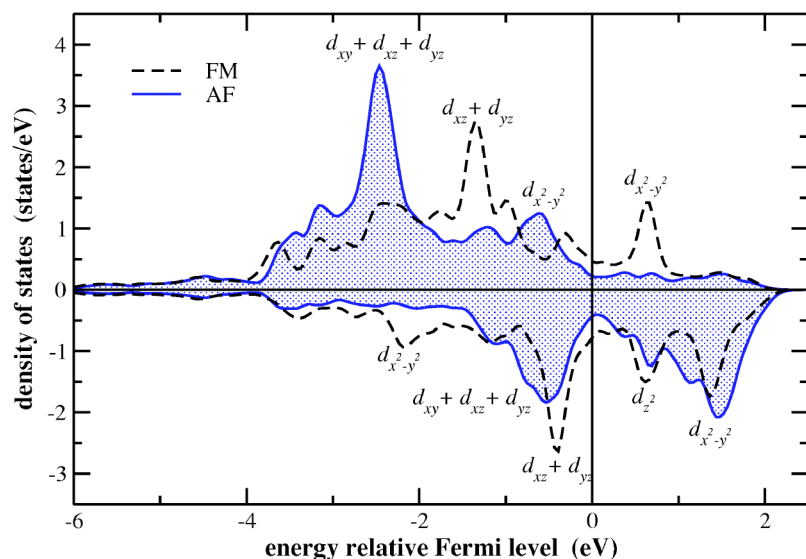
FIG. 2. (Color online) Density of states projected onto Fe atom in ferromagnetic (FM) and antiferromagnetic (AF) Fe/W(100) films.

AF ground state is due solely to hybridisation with tungsten atoms. Furthermore, the charge in the muffin-tin sphere around an Fe atom increases by nearly $0.7e$ in an Fe/W(100) overlayer compared to the free-standing monolayer. This could indicate a massive charge redistribution at the Fe/W interface, but a detailed analysis of the charge distribution reveals that the muffin-tin spheres around all W atoms, including those at the interface contain practically the same charge before and after deposition of an Fe monolayer onto a clean surface. This means that the charge spilling out into the vacuum in a free-standing Fe monolayer is considerably reduced in the Fe/W(100) adlayer and that this charge remains largely within the adlayer. Such an analysis suffers from the drawback that the partitioning of the total charge among separate atoms by means of projection on *ad hoc* chosen atomic spheres is a slightly ambiguous procedure, yet it gives at least a hint that the Fe-W bonding is of covalent rather than ionic character in addition to the expected metallic bonding. Regarding the relaxed equilibrium geometry of the Fe/W(100) monolayer, we find a heavy magnetoelastic effect—the Fe-W interlayer spacing expands by 0.2 Å when a nonmagnetic film assumes a $c(2 \times 2)$ AF order.

In 2-ML Fe/W(100) films the FM state is preferred, see Table III. These results correlate nicely with MOKE experiments,[15] which reported a Curie temperature of $T_C = 323$ K for a 1.5-ML film, whereas for near-monolayer coverage no vestige of magnetisation was detected down to 115 K. In a recent study of Fe/W(100) films by Wulfhekel *et al.*[16] the Kerr ellipticity at remanence has been measured as a function of coverage. A linear dependence has been obtained with zero Kerr ellipticity at slightly above one ML of Fe. This behavior has been interpreted as a quenching of the magnetic moment in the Fe monolayer. On the basis of our calculations the absence of a MOKE signal is due to the AF ordering. The individual atoms carry large magnetic moments which should be easily detectable by local techniques such as Mössbauer spectroscopy. We are unaware of any such experiments, though. Further, we have examined the possibility of a reconstruction of the Fe adlayer, similar to the patterns explored for the W(100) surface. However, none

of these attempts led to a destabilization of the simple pseudomorphic Fe-W relationship. Upon Fe coverage the W(100) surface dereconstructs back to a (1×1) surface symmetry, irrespective of the magnetic state of the adlayer. Below we show that even a single Fe adatom can locally alleviate the W(100) reconstruction very efficiently.

The Fe/W(110) films present a simpler picture—both 1-ML and 2-ML films are ferromagnetic. As to the 1-ML thick film, the antiferromagnetic configurations represent metastable solutions. Our values for the ferromagnetic moment of $2.41\mu_B$ and the downward relaxation by 14.7% agree well with the experimental estimate, $m = 2.53 \pm 0.12\mu_B$ (Ref. 18), and theoretical results by Qian and Hübner,[31] $m = 2.54\mu_B$ and $\delta_{12} = -12.9\%$, whereas the other two studies[29,30] yield a larger relaxation accompanied by a more pronounced reduction of magnetic moment. This points to a close correlation between the size of magnetic moment and the position of the Fe layer above the substrate and hence to strong hybridization effects. The difference in the topmost interlayer distance is most likely caused by application of gradient corrections to the exchange-correlation functional in our calculation and in Ref. 31, whereas these corrections were not included in Refs. 29 and 30. The gradient corrections are known to cure the problem of overbonding in the local-density approximation

TABLE III. The same structural, magnetic and energetical parameters as in Table II, but for 2-ML Fe films on W(100) and W(110) surfaces. Abbreviation AF stands for a layer-antiferromagnetic alignment.

	δ_{12} (%)	δ_{23} (%)	δ_{34} (%)	m_1 (μ_B)	m_2 (μ_B)	ΔE_m (meV)
2Fe/W(100)-FM	−28.8	−14.9	0.6	2.71	1.81	0
2Fe/W(100)-AF	−32.5	−16.4	0.7	−2.67	1.48	123
2Fe/W(100)-NM	−42.1	−14.4	2.7	0.00	0.00	341
2Fe/W(110)-FM	−23.7	−10.9	−1.0	2.84	2.15	0
2Fe/W(110)-AF	−20.1	−13.1	−0.5	−2.84	1.64	240
2Fe/W(110)-NM	−39.2	−9.8	−1.3	0.00	0.00	514

and to stabilize the FM bcc ground state of bulk Fe, whereas calculations without GGA predict Fe to be nonmagnetic and hexagonal close packed.[50] The changes in the subsurface interlayer distances are very modest, as expected for a metal with very high cohesion.

Structural characterization by LEED demonstrated a relaxation of the Fe-W interlayer spacing by $\delta_{12}=-13\%$ (Ref. 22). A somewhat smaller contraction of $\delta_{12}=-8\%$ has been found using interface-specific photoelectron diffraction.[23] All these measured data are perfectly reproduced by our calculations within the experimental error bars. Moreover there is a very good agreement with the results obtained previously by a different density-functional approach, the full-potential linearized augmented wave method employing the generalized gradient corrections.[31] The magnetic moments induced at the W interface atoms do not exceed $0.16\mu_B$ and therefore they are not specified in detail. We just note that they are antiparallel with respect to dominant Fe moments in a ferromagnetic solution.

The Fe-Fe interlayer spacings in FM 2-ML films are $d_{12}^{[100]}=1.13$ Å and $d_{12}^{[110]}=1.72$ Å. Using the calculated lattice parameter of FM iron, $a_{Fe}=2.83$ Å, these values can be related to the interlayer spacing in bulk Fe strained to match the W substrate. Assuming volume conservation one calculates $d_{12}^{[100]}=1.12$ Å and $d_{12}^{[110]}=1.58$ Å. The former value is almost precisely equal to that found in 2-ML Fe/W(100) film and hence this film has the same volume per atom as bulk iron. On the other hand, the atomic volume in 2-ML Fe/W(110) film is expanded by 9%.

V. ENERGETICS OF SURFACE DIFFUSION

In the preceding section we concentrated on the characterization of the structural and magnetic properties of thin Fe films at thermodynamic equilibrium. However, under realistic experimental conditions this equilibrium cannot be always achieved, due to various kinetic limitations. For the understanding of film growth the knowledge of the surface diffusion constant is required. To this end we calculated the activation energy barriers for hopping processes between two adsorption sites for Fe adatoms on the W(100) and W(110) surfaces and the energy associated with exchange-diffusion processes. The activation energy barrier is defined as the difference between the saddle point (or transition state) energy and the energy of the stable adsorption site. Analogous calculations have been performed for migrating Fe adatoms and vacancies on Fe/W(100) and Fe/W(110) overlayers. Finally we will discuss diffusion processes along steps on a vicinal W(420) surface. Unless stated explicitly, the adatoms and films were assumed to be nonmagnetic. This seems to be justified as diffusion is a temperature-activated process and the magnetic transition temperatures of ultrathin Fe films are around or below room temperature.

A. Diffusion of Fe on W(100) and W(110) surfaces

Basically, an adatom on a surface moves either by random jumps to a near vacant binding site or by an exchange process replacing an atom in the underlying lattice which is
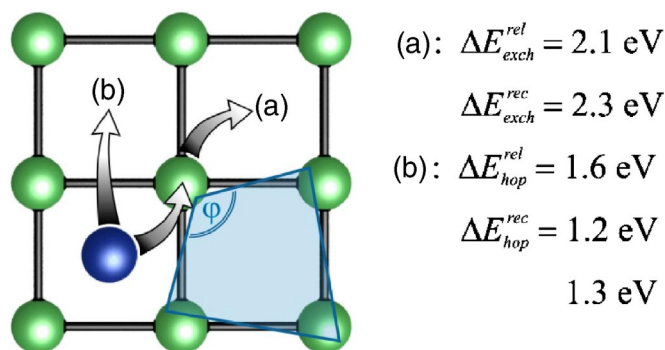

FIG. 3. (Color online) Top view of the Fe adatom (the darker ball) on W(100) surface. The arrows show possible jump and exchange processes for which the energy barriers ΔE have been obtained. The semitransparent deltoid marks the local geometry of reconstructed W(100) surface. The two values for the energy barriers on the reconstructed surface refer to hopping across the longer and shorter sides of the deltoid.

pushed out to the surface.[51,52] On the W(100) the most favorable adsorption site for an Fe adatom is in the fourfold hollow. The adsorption energy is 0.22 eV and the Fe atom is located 0.87 Å above the reconstructed surface; for the relaxed surface the adsorption energy amounts to 1.43 eV and the Fe atom is 0.83 Å above the surface, indicating by far more favorable adsorption conditions at the relaxed surface. In the definition of the adsorption energy as an energy difference of the surface with adsorbed atom and the clean surface plus free adsorbate we have taken as the reference energy of the free adsorbate the cohesive energy of a Fe atom in nonmagnetic bcc iron bulk. The exchange process of a Fe adatom with one of neighboring surface W atoms is highly improbable due to a significant energy barrier of ΔE_{exch}^{rec} =2.3 eV or ΔE_{exch}^{rel}=2.1 eV for the reconstructed or the relaxed W(100) surface, respectively. We remark that the final configuration with one Fe atom incorporated in the surface and one ejected W atom has in fact an energy lower by 109 meV (for the reconstructed phase) or by 268 meV (for the relaxed phase), and hence this configuration is thermodynamically stable. The activation energy of a hopping process on the relaxed W(100) surface is also quite high, ΔE_{hop}^{rel} =1.6 eV. Smaller values were obtained for Fe adatoms moving on the reconstructed W(100) surface. As the symmetry of this surface is lower, one has to distinguish jump events over the longer and shorter side of a deltoid as sketched in Fig. 3. Were the activation energies along these two directions very different, adatoms would diffuse preferentially along the [011] directions. This is not the case because we find much the same energy barriers of 1.2–1.3 eV along both directions, so that the diffusion happens by uncorrelated random walk. The reason why the two energy barriers do not differ appreciably is the modification of the local surface geometry induced by an Fe adatom. The distortion of the nearest-neighbor squares on the reconstructed surface can be characterized by an obtuse angle in the resulting deltoid of φ =106°, see Fig. 3. Adding an Fe atom above the center of such a deltoid reduces the distortion to φ=95°, i.e., the square symmetry is almost completely restored on a local

(a): $\Delta E_{exch}^{[00\bar{1}]} = 2.9$ eV

(b): $\Delta E_{exch}^{[1\bar{1}0]} = 4.2$ eV

(c): $\Delta E_{hop}^{[\bar{1}11]} = 0.7$ eV

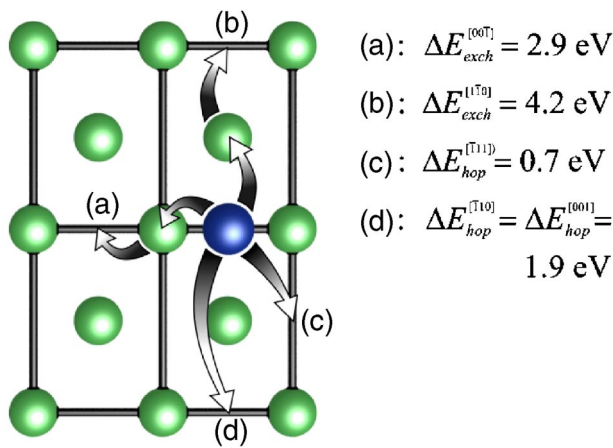(d): $\Delta E_{hop}^{[\bar{1}10]} = \Delta E_{hop}^{[001]} = 1.9$ eV

FIG. 4. (Color online) The same as in Fig. 3 but for an Fe adatom on the W(110) surface.

scale. The same mechanism of a local dereconstruction of the W(100) surface applies to Fe atoms incorporated in the surface. Therefore the energies connected to the exchange process on the reconstructed and relaxed surfaces are quite similar. We can conclude that the kinetics of Fe surface diffusion is governed by the hopping process. The exchange and hopping processes for an Fe adatom on the W(100) surface and the corresponding energy barriers are summarized in Fig. 3.

The activation energies for the diffusion of an Fe adatom on the densely packed W(110) surface are reported in Fig. 4. The stable adsorption site is along the long bridge between two surface atoms at a height of 1.71 Å, the adsorption energy is 0.10 eV. The threefold adsorption site turns out to be unstable, and the short bridge site represents a transition state with an energy increased by 0.7 eV compared to the long bridge position. The exchange processes along both inequivalent directions are disfavored by extremely high activation energies. The reason for the high barriers for exchange diffusion is the strong binding between the W atoms in this closed-packed surface. In contrast to the W(100) surface the configuration with the Fe adatom in the long bridge position above the surface is nearly 1 eV more stable than the configuration with an embedded Fe atom. The jumps to the next-nearest neighbor sites appear also unlikely as they are associated with energy barriers of 1.9 eV. The sole relevant process for surface diffusion of Fe adatoms on W(110) are the short jumps to vacant adsorption sites at nearest neighbor distance, as they have a modest hopping energy barrier of 0.7 eV. This value is in good agreement with the measured activation energy of diffusion of 0.6 eV (Ref. 21). Relatively moderate hopping and huge exchange energy barriers favor the formation of atomically smooth Fe/W(110) overlayers. Experimentally it has been demonstrated that these films are one of the best examples of truly two-dimensional magnetic systems.[28]

B. Diffusion of adatoms on Fe/W films

The first layer of iron on both W(100) and W(110) surfaces grows pseudomorphically despite a relatively large 9.4% misfit with the substrate. On the W(110) surface misfit

dislocations are created at coverages ranging from 1.2 (at 570 K) to 1.8 ML (at ambient temperatures) to compensate for the large strain.[19,26] The strain relaxation in Fe/W(100) films is delayed up to 4 ML at 400 K.[16] Annealing to higher temperatures leads to the formation of fully relaxed islands on top of a 2-ML thick pseudomorphic "carpet".[13] To comprehend the differences in the growth of 2-ML thick films on the two different tungsten surfaces we identify the adsorption sites and analyze the migration of Fe adatoms on 1-ML Fe-covered tungsten.

1. Diffusion of Fe on Fe/W(100) films

We present the results for nonmagnetic Fe/W(100) films first. Our starting assumption was that an Fe adatom will be located in a fourfold hollow of the Fe overlayer, but for the hopping barrier from one hollow site to the next one we obtained a negative energy barrier, meaning that Fe adsorbs preferentially at a bridge position. This is a very surprising result, because as a rule metal atoms tend to adsorb at the highest coordination sites. On the path from the hollow to the bridge site the energy decreases continuously, implying that the hollow site represents an unstable adsorption configuration. In the optimized bridge geometry the Fe adatom is located at 0.91 Å above the plane of the Fe film and the bond length to its two neighbors is 2.17 Å. The adsorption energy is 0.46 eV. From the dependence of the energy difference between the bridge and hollow adsorption site on the coverage displayed in Fig. 5 it follows that the hollow adsorption sites are favored only at a coverage higher than 0.43 ML. The structure of a complete 2-ML film corresponds to the usual pseudomorphic relationship with the substrate. In this analysis we assumed a uniform distribution of the Fe atoms at every coverage. This does not reflect the formation of close-packed islands taking place in a submonolayer range. Nevertheless, Fig. 5 convincingly illustrates the trend from the preferred bridge adsorption site for an isolated adatom to the hollow adsorption site with increasing Fe-Fe interactions. The energies of hopping and exchange processes of Fe adatom located at the bridge position are summarized in Fig. 6. The shortest bridge-bridge hopping process with an activation energy of $\Delta E_{hop}^{[011]} = 0.4$ eV is obviously the favored migration mechanism, but jumps to next-nearest bridge places require only a slightly higher activation energy of $\Delta E_{hop}^{[0\bar{1}1]} = 0.5$ eV. Exchange diffusion also has a surprisingly low activation energy of 0.7 eV.

In Sec. IV we arrived at the conclusion that a 1-ML Fe/W(100) film assumes an AF order. Because the Néel temperature is not known and potentially high enough to matter, we explored how the magnetic state will change the picture outlined above for a nonmagnetic film. The magnetic state has a profound influence on the preferred adsorption site and also on the kinetics of surface diffusion. The situation is complicated by the fact that the magnetic interaction of the adatom with the $c(2 \times 2)$ AF film necessarily introduces some degree of frustration. If one assumes that the deposition of the adatom does not change the AF ordering of the underlying film, an adsorbed Fe atom occupies the hollow position 1.17 Å above the film and has an adsorption energy of 0.40 eV. The
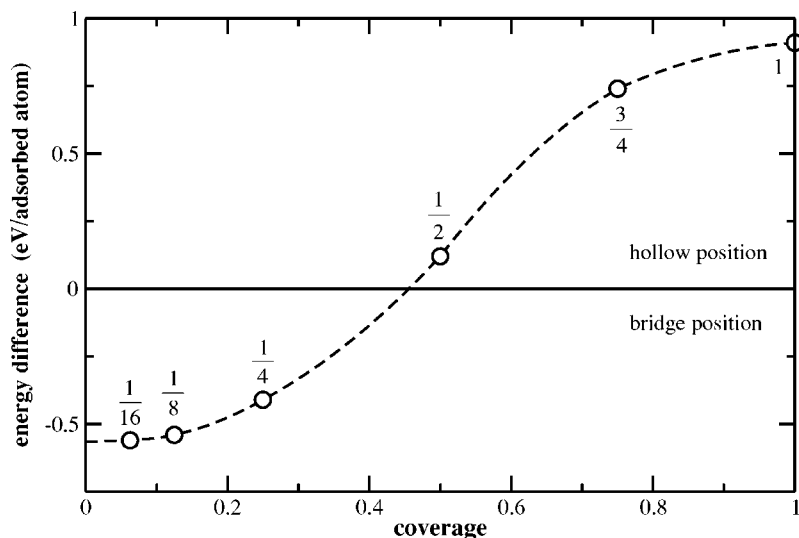
FIG. 5. Energy difference between the bridge and hollow adsorption sites of Fe adatom on nonmagnetic 1-ML Fe/W(100) film as a function of coverage. The dashed line serves as a guide to the eye.

magnetic moments of the adatom is 2.76 μ_B, the magnetic moments of the four nearest neighbors in the underlying film are reduced to 2.14 μ_B for the two atoms coupling ferromagnetically to the adatom and to -1.87 μ_B for atoms with the oppositely aligned moments, see Fig. 7(a). However, the bridge position is disfavored by merely 0.1 eV, the magnetic structure of the transition state is shown in Fig. 7(b). Hence the adatom can visit both positions with almost equal probability. An intriguing implication of this result is the prediction that the diffusion of Fe adatoms on an Fe/W(100) film becomes much faster after the film is cooled down below the Néel temperature. The extraordinarily smooth potential energy surface experienced by the Fe adatom can be understood in terms of frustrated magnetic interactions with AF underlayer. The magnetic moment of an Fe adatom in the hollow and the bridge sites is 2.76 μ_B and 2.59 μ_B, respectively. These values are very close to the surface magnetic moment of 2-ML Fe/W(100) films, $m_1 = 2.71$ μ_B. In fact, because of the reduced coordination of the Fe adatom in the bridge site, an increased magnetic moment would be expected. However, this is not the case because of competing interactions with the surface atoms. In the transition state the magnetic moments of the Fe atoms in the film interacting with the adatom are

very strongly quenched, but the moments of their neighbors relax to values close to those in the clean film, see Fig. 7(b). In the hollow site all four magnetic moments below Fe adatom are reduced with a more pronounced reduction occurring for antiparallel moments. Thus, the interaction of an Fe adatom with its neighbors is predominantly ferromagnetic. The strong reduction of the moments reduces the frustration within the film, leading to the surprisingly low diffusion barrier.

Because of the preferred FM interactions of the adatom with the underlayer, it seems reasonable to expect that before a completion of 2-ML films ferromagnetic 2-ML thick islands are built which coexist with antiferromagnetically ordered uncovered regions. Experiments have indeed detected ferromagnetic order for a 1.5-ML thick films.[15,16] We have explored the possibility that an Fe adatom in a hollow position induces a locally ferromagnetic configuration such as shown in Fig. 7(c). Although this leads to an increase of the number of frustrated nearest-neighbor interactions (four within the Fe films instead of two between adatom and AF substrate), the total energy is lower by 0.3 eV than for an adatom on the AF film. The magnetic moment of the adatom is also increased, and the reduction of the moment in the film is only modest. The problem with this configuration is that the diffusion of the adatom is accompanied by a spin-reorientation on the neighboring sites, and this leads to considerable complications in the transition-state search. Most certainly, the magnetic state of the transition state consists of a canted spin configuration. To explore this possibility goes beyond the scope of the present work. To get at least a semi-quantitative estimate of the diffusion barrier, we have calculated the potential energy of the adatom in the bridge position with a fixed direction of the magnetic moments. Again the moments on the sites forming the bridge are reduced [see Fig. 7(d)], but not as strongly as in the case of an AF film. The calculated barrier height is 0.3 eV. The moments belonging to the atoms of the FM island left behind by the migrating atom increase even slightly, indicating that the energy of formation of a magnetic defect is not very large. The actual barrier height might be somewhat different (asymmetry of the transition state, spin canting), but it is evident that

(a): $\Delta E_{exch} = 0.7$ eV

(b): $\Delta E_{hop}^{[001]} = 0.5$ eV

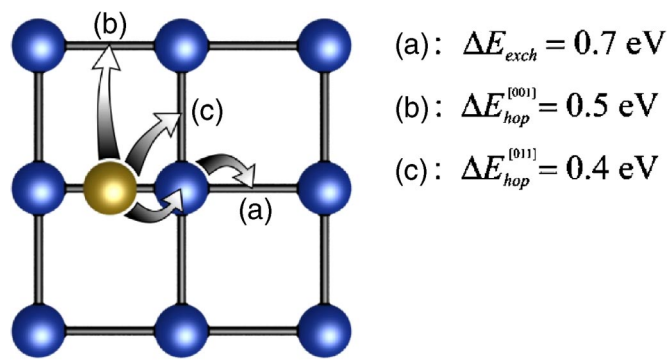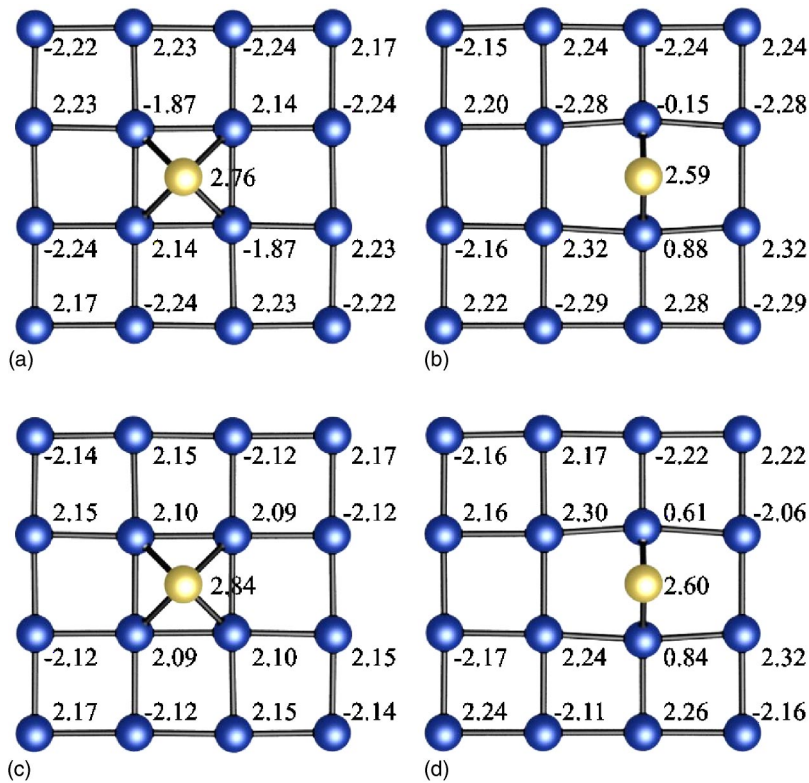(c): $\Delta E_{hop}^{[011]} = 0.4$ eV

FIG. 6. (Color online) Top view of Fe adatom (the brighter ball) adsorbed on 1-ML Fe/W(100) film. The examined diffusion processes and the related energy barriers are presented.

FIG. 7. (Color online) Magnetic configurations of Fe adatoms on Fe/W(100) layers. (a) Fe on $c(2\times2)$ AF Fe/W(100), (b) transition state for Fe diffusion on AF Fe/W(100), (c) Fe adatom forming a local FM defect on the $c(2\times2)$ AF film, (d) transition state for Fe diffusion on a film with a magnetic defect.

the activation energy for the diffusion of an adatom on the magnetic film will be lower that on a nonmagnetic film, reverting the temperature dependence of the diffusion rates.

We have also estimated the energy barrier for an exchange of an adatom with a neighboring atom in the AF film [see Fig. 7(a)] carrying parallel or antiparallel magnetic moment. In the former case $\Delta E_{exch}=0.7$ eV was estimated from the calculation of the energy change along the full transition path. The exchange process of an AF coupled pair of Fe atoms is more complex, because between the initial and final states both atoms have to flip their magnetic moments and at the transition state one probably has a canted magnetic configuration. We have chosen to examine two simpler approximations to the transition state, the first one with antiparallel moments of the exchanging atoms, and the second one with zero initial magnetic moments (which developed to a transition state with small parallel moments of about 0.2 μ_B) of the exchanging atoms. In the first case we got $\Delta E_{exch}=0.9$ eV, whereas the second scenario yields to $\Delta E_{exch}=1.3$ eV. Therefore it can be concluded that the exchange process of atoms carrying parallel magnetic moments is more probable, which in turn means that the diffusion via an exchange process of a single magnetic adatom over an AF surface is anisotropic with the fast direction along the [011] direction. However, the dominant mechanism for Fe diffusion on Fe/W(100) adlayer remains the hopping process, irrespective of the magnetic state.

2. Diffusion of Fe on Fe/W(110) films

Next, we address atomic motion on nonmagnetic Fe/W(110) films. An Fe adatom adsorbs preferentially at a long bridge site 0.83 Å above the surface plane and has an adsorption energy of 0.99 eV. For the hopping from one long bridge site to a neighboring long bridge site a large barrier $\Delta E_{hop}^{[111]}=1.4$ eV is calculated. For the exchange with a nearest neighbor along the [001] direction we obtain $\Delta E_{exch}^{[001]}=0.5$ eV. Quite surprisingly, for the exchange along the $[\bar{1}10]$ direction $\Delta E_{exch}^{[\bar{1}10]}=-0.7$ eV and hence the pseudomorphic 1-ML Fe/W(110) film with an Fe adatom is unstable. The evolution of the adsorption energy along the transition path and the final structure resulting from the exchange process are shown in Fig. 8. The film can be characterized as two-dimensional with two atoms forming a sort of slightly protruding dimer with a buckling amplitude of 0.19 Å. It is conceivable that such a geometry locally relieves the lattice strain accumulated in a pseudomorphic Fe monolayer, it can be considered as a step towards the formation of a close-packed overlayer with complete or incomplete misfit dislocation such as it has been reported for Co/W(110) near monolayer coverage.[53] However, experimental studies[19,26] report the appearance of a dislocation network and hence the loss of the pseudomorphic film-substrate relationship only for a coverage exceeding 1.2 ML. With one adatom per (4×3) surface cell, the nominal coverage is 1.04 ML and it is not unrealistic to assume that a local loss of pseudomorphicity starts already at this coverage. In this respect we would like to allude to the work by Nahm and Gomer.[20] They observed two distinct forms of Fe/W(110) overlayers with very different work functions Φ; a smaller one, $\Phi=4.5$ eV, for films deposited at 90 K and a larger one, $\Phi=4.8$ eV, for films prepared at 300 K. As the more dense surfaces generally have a larger work function[39] it is appealing to associate our distorted structure with a higher-temperature phase from Ref. 20. Indeed, the calculated work function of nonmag-
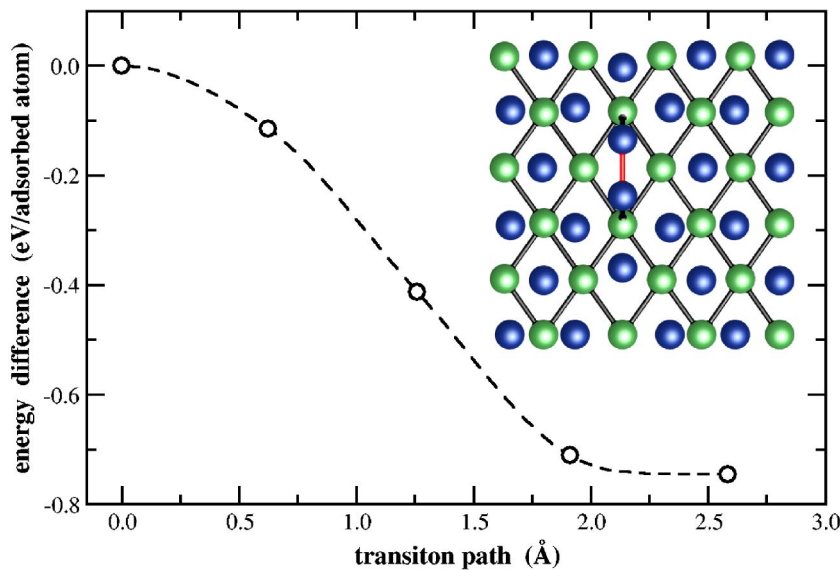
FIG. 8. (Color online) The transition path of Fe adatom on 1-ML Fe/W(110) film migrating from the long bridge site and pushing out the adjacent atom beneath along the $[\bar{1}10]$ azimuth. The exchange process is not completed, as both participating atoms form a dimer immersed in the surface layer. The resulting geometry is displayed in the inset. The length of the Fe-Fe dimer is 2.28 Å, the shortest Fe-W bond length is 2.36 Å.

netic, pseudomorphic Fe/W(110) adlayer equals 4.3 eV which is closer to a low-temperature (arguably metastable) form. However, both phases observed in Ref. 20 are claimed to have a (1×1) symmetry seen by LEED, therefore such an assignment can be questioned. Furthermore, we have explored structural models suggested in Ref. 20, in which the Fe layer in 1-ML Fe film is misaligned with respect to the substrate (e.g., adsorption sites are quasi-threefold instead of twofold ones), but these geometries turned out to be unstable in our calculations. Obviously, there is much that still needs to be learned regarding the morphology of 1-ML Fe/W(110) films. The existing STM investigations[26] were able to observe the onset of island coalescence in a submonolayer regime, and of a dislocation network between 1 and 2 ML, but atomic-scale details were not provided owing to insufficient corrugation of the local density of states in the Fe layer. The lack of atomically resolved structural information on 1-ML thick films prevents us from attaining a more detailed atomistic description of diffusion mechanisms of Fe adatoms on Fe/W(110) films.

Our present results suggest that the Fe adatoms on a 1-ML Fe/W(110) film are incorporated in the Fe layer, forming an interstitial dumbbell as a nucleus of a close-packed overlayer. The activation energy for the migration of this defect is just equal to the energy difference between this configuration and the adatom in the long bridge site $\Delta E = 0.7$ eV.

C. Vacancy diffusion in Fe/W(110) and Fe/W(110) films

In an almost complete Fe overlayer diffusion proceeds mainly via migration of vacancies. As we have shown in Sec. V A the Fe-W exchange processes cost too much energy to take place, therefore in the study of vacancy diffusion we restrict ourselves to the simplest mechanism, direct jumps. The vacancy formation energies amount to 0.74 and 0.10 eV for the nonmagnetic Fe/W(100) and Fe/W(110) films, respectively. For vacancy diffusion in a nonmagnetic 1-ML Fe/W(100) film we obtained $\Delta E_{\text{hop}}^{[001]} = 2.0$ eV, and if the AF

ground state is accounted for $\Delta E_{\text{hop}}^{[001]} = 2.1$ eV. Among the three vacancy migration processes in Fe/W(110) overlayer, displayed in Fig. 9, the shortest jump-path along the $[\bar{1}11]$ direction is connected with the smallest energy barrier, $\Delta E_{\text{hop}}^{[\bar{1}11]} = 0.6$ eV, but hopping along the $[\bar{1}10]$ directions can contribute to vacancy diffusion as well ($\Delta E_{\text{hop}}^{[\bar{1}10]} = 0.7$ eV). Note that our computational models correspond to Fe films with 6% [on W(100)] and 4% [on W(110)] of vacancies rather than a single vacancy, but we do not expect any significant deviations from the calculated energy barriers due to vacancy-vacancy correlations present in our models.

A remarkable result is that for Fe/W(100) films adatom diffusion is much faster than vacancy diffusion. Hence vacant sites can be filled only by migrating adatoms, the point defect cannot be eliminated by migration to the boundary of the growing film. For Fe/W(110) vacancy migration is pre-

(a): $\Delta E_{hop}^{[\bar{1}11]} = 0.6$ eV

(b): $\Delta E_{hop}^{[\bar{1}10]} = 0.7$ eV

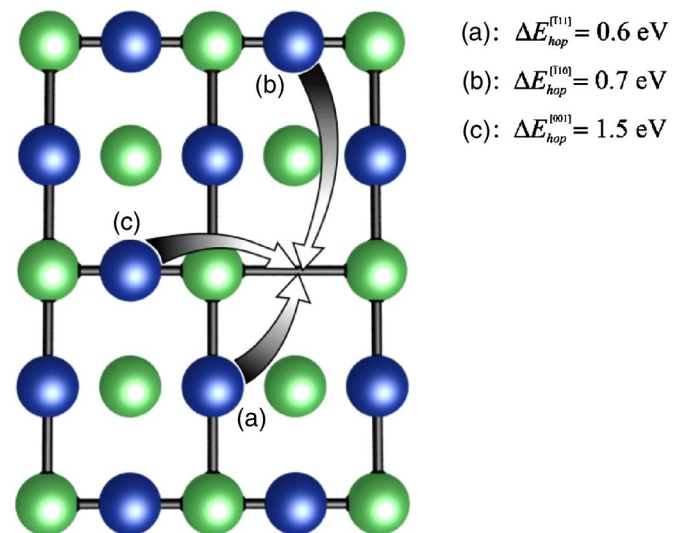(c): $\Delta E_{hop}^{[001]} = 1.5$ eV

FIG. 9. (Color online) Top view of 1-ML Fe/W(110) film with one vacant site to be filled with one of the adjacent atoms. The respective energy barriers are provided.

(a) : $\Delta E_{hop} = 1.5$ eV

(b) : $\Delta E_{hop} = 1.3$ eV

(c) : $\Delta E_{exch} = 1.5$ eV

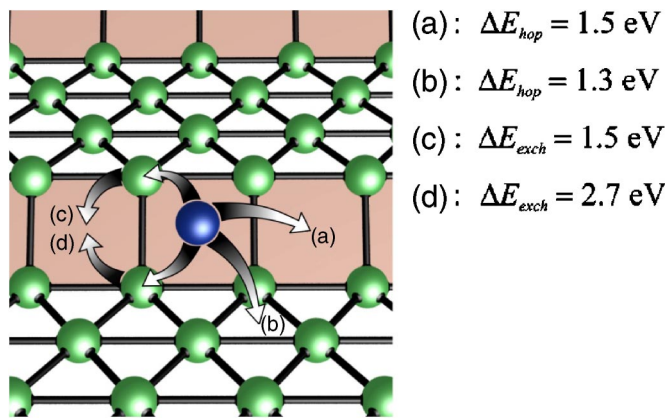(d) : $\Delta E_{exch} = 2.7$ eV

FIG. 10. (Color online) Oblique view of W(420) surface with various diffusion processes of Fe adatom near a step. The step facet is highlighted. The calculated energy barriers are presented.

dicted to be quite fast, whereas adatoms can disrupt locally the pseudomorphic relationship with the substrate.

D. Diffusion of Fe atoms near steps

Microscopic information on atom migration along steps can be very helpful for a better understanding of film growth. The homoepitaxial growth mode (flat versus rough) and the shape of islands (compact versus dendritic islands) are mostly determined by self-diffusion along edges. For heteroepitaxy, such as Fe atoms on a W surface in our case, the diffusion along the steps can be faster or slower than diffusion across flat surfaces. In the former case a preferential formation of step-decorating stripes will occur, whereas in the latter case Fe atoms near the edges become immobile and serve as nucleation centers for island growth near the edges. However, for reliable predictions concerning the roughness of Fe stripes along edges many other processes must be taken into consideration. For instance, a low diffusion barrier for a single Fe atom along a row of Fe atoms attached to a step will give rise to a smooth stripe geometry.

Steps with various orientations are present on tungsten surfaces. In this study we consider a W(420) surface, i.e., the $4(110) \times (100)$ surface in the compact notation.[54] It is a (110) vicinal surface with (110) terraces consisting of four rows of atoms and with ⟨100⟩-type steps. We have repeated the basic unit cell five times along the steps so that migrating adatoms are 15.9 and 9.3 Å apart from each other along and across the steps, respectively. The four explored migration processes together with the calculated energy barriers are presented in Fig. 10. The hopping process denoted as (b) from the fivefold hollow on the edge microfacet to a long bridge hollow terrace position has the smallest energy barrier of 1.3 eV. Because the starting configuration is more stable by 0.8 eV than the final configuration (the adsorption energies are 1.09 and 0.29 eV for the starting and the final configurations, respectively), during the reverse jump from the terrace to the edge an Fe atom has to surmount only an energy barrier of 0.5 eV. Diffusion along the step, from one fivefold hollow to the next one [process (a)] requires an activation energy of 1.5 eV. The exchange mechanism denoted by (c)

of Fig. 10 has a comparable activation energy and it is interesting to note that the final configuration in this process, in which the Fe atom is integrated into the outer edge corner, has an energy higher only by 0.1 eV compared to the initial configuration. Recalling that the exchange process on a flat (110) surface has an activation energy $\Delta E_{exch} = 2.9$ eV, it is obvious that a moderate surface alloying of Fe on W at high temperatures starts at the step edges.

The smallest diffusion barrier found at flat W(110) surface amounts to 0.7 eV. This indicates that an Fe atom arriving at a step will be more or less trapped there because of its higher binding energy at the step edge or eventually will diffuse along the step at a slower pace than the atoms on the terrace.

We explored also the distinct case of an Fe adatom diffusing along steps decorated by one row of Fe atoms. For the same migration processes as those displayed in Fig. 10 we find $\Delta E_{hop}^{(a)} = 1.1$ eV, $\Delta E_{hop}^{(b)} = 0.9$ eV, $\Delta E_{exch}^{(c)} = 1.0$ eV, $\Delta E_{exch}^{(d)} = 2.4$ eV. Obviously, the energy barriers are decreased as can be expected because it is easier to break an Fe-Fe bond then a W-W bond. The same trend has been seen in the study of Fe diffusion on clean and Fe-covered W(100) surfaces (see Figs. 3 and 6). The difference between the binding site at the step edge and the long bridge site (b) drops to 0.1 eV. All in all, diffusion along decorated steps and flat portions of surfaces is governed by comparable activation energies within the limits of our accuracy, in agreement with the results of spreading experiment.[36]

VI. DISCUSSION AND CONCLUDING REMARKS

We have presented an extended *ab initio* DFT investigation of the structure of clean W(100) and W(110) surfaces, of the structure and magnetic properties of Fe/W(100) and Fe/W(110) films, and of the diffusion of Fe atoms and vacancies on flat and stepped surfaces and films. Our investigations of the clean tungsten surfaces are in good agreement with previous studies of these surfaces based on semilocal (gradient-corrected) exchange-correlation functionals. We have examined in particular the reconstruction of the W(100) surfaces and have found that neither the surface energy nor the surface stress reach a minimum at the fully reconstructed state. We argue that a local-bonding model is the most appropriate description of the reconstruction mechanism.

Experimental studies usually describe 1-ML films of Fe on W(100) as nonmagnetic—we find a $c(2 \times 2)$ AF ground state on a dereconstructed W(100) surface. Our investigations of isolated Fe adatoms on the reconstructed W(100) demonstrate that already the adsorption of an isolated Fe largely relieves the distortion of the surface geometry. 2-ML Fe/W(100) films are predicted to be ferromagnetic, in agreement with experiment. Here again we find that even an isolated Fe adatom on top of an antiferromagnetic 1-ML Fe film induces the formation of a ferromagnetic defect in coexistence with antiferromagnetically ordered uncovered regions. The situation is much simpler for Fe films on W(110) substrates. Both 1-ML and 2-ML films are ferromagnetic, with Fe moments that are slightly higher than in bulk iron, but lower than on an iron surface. Both the magnetic and the structural data agree very well

with experiment—provided that gradient corrected functionals are used.

The main subject of our work, however, is the diffusion of Fe adatoms and vacancies on the clean tungsten surfaces and on Fe/W films. On W(100), the adsorption energy of Fe is considerably larger on the relaxed than on the reconstructed surface. In fact, even the adsorption of a single adatom largely relieves the local strains and initiates dereconstruction. Fe diffusion on W(100) proceeds by a hopping process, the activation energy is lower on the reconstructed than on the ideal surface. Diffusion is predicted to be almost isotropic. An exchange process leading to the incorporation of the Fe atom in the W surface and the formation of a W adatom is a slightly exothermic process, but is inhibited by a high activation energy of more than 2 eV. On the W(110) surface the preferred diffusion path is via nearest-neighbor hopping between long bridge sites. Exchange diffusion is found to have a prohibitively high activation energy, in accordance with the strong binding within this close-packed tungsten surface.

The results for the diffusion of adatoms on monolayer Fe films offer some very interesting facets. For the Fe/W(100) films we have considered diffusion both in the nonmagnetic high-temperature and in the antiferromagnetic low-temperature regimes. On the nonmagnetic Fe films, the stable adsorption site for the adatom is not the hollow, as naively expected for pseudomorphic growth, but the bridge site. Activation energies for both nearest- and next-nearest-neighbor hopping processes are rather low, 0.4 and 0.5 eV respectively. On the antiferromagnetically ordered film, the potential energy surface for adatom diffusion is very flat, but we find that the adsorption of an Fe atom induces the formation of a magnetic defect in form of a ferromagnetically coupled island—this agrees with the observation that the antiferromagnetic to ferromagnetic transition is initiated already at coverages of about 1.5 ML. Diffusion of the adatom is hence coupled to local spin-reorientations in the film and this makes it extremely difficult to estimate the activation energy. Still, our results are consistent with the surprising fact that diffusion on the magnetically ordered films at low temperatures should be faster than on a nonmagnetic film at high temperature. The investigation of exchange diffusion on 1-ML/W(110) film leads to the prediction that even an isolated adatom destabilizes the pseudomorphic structure of the film—the adatom is incorporated in the film and forms the nucleus of a close-packed film with misfit dislocations.

Vacancy diffusion in an Fe/W(100) film is predicted to have a high activation energy of about 2 eV, irrespective of the magnetic state of the film. For Fe/W(110) we predict a low vacancy formation energy and an activation energy for vacancy diffusion comparable to that for Fe adatom diffusion. These results indicate that while in Fe/W(100) point defects can be annihilated only by the trapping of diffusing adatoms, in Fe/W(110) the high mobility of both adatoms and vacancies facilitates the formation of compact, defect-free adlayers.

Our study has been completed by the investigation of diffusion along ⟨100⟩ steps on a clean W(110) surface film and on an Fe/W(110) film. On the clean surface, the activation energy for diffusion along the edges is distinctly higher than diffusion on the terraces and the adsorption near an edge is preferred compared to the adsorption on terrace sites, implying that Fe adatoms will be trapped at the step edges. If the steps are decorated by monoatomic Fe wires, the activation energies for step diffusion are reduced and become comparable with those for Fe diffusion on terraces.

In summary, our investigations have shown that there is a strong correlation between structure, magnetism and atomic dynamics in nanostructured Fe/W magnets. To the best of our knowledge, this is the first *ab initio* study of diffusion on magnetic thin film systems. For Fe on a W(110) template, our calculated activation energies are in very good agreement with the available experimental data—this is an important validation of *ab initio* DFT studies of diffusion. For Fe diffusion on W(100) the reconstruction and local dereconstruction play an important role in determining the activation energy. For Fe diffusion on 1-ML Fe/W(100) the magnetic frustration introduced in the antiferromagnetic film leads to a strongly reduced corrugation of the potential energy surface and the surprising prediction that magnetic ordering is the cause of enhanced diffusion.

---

*Email address: Daniel.Spisak@univie.ac.at

[1] K. Yonehara and L. D. Schmidt, Surf. Sci. **25**, 238 (1971).

[2] T. E. Felter, R. A. Barker, and P. J. Estrup, Phys. Rev. Lett. **38**, 1138 (1977).

[3] M. K. Debe and D. A. King, Phys. Rev. Lett. **39**, 708 (1977).

[4] A. Fasolino, G. Santoro, and E. Tosatti, Phys. Rev. Lett. **44**, 1684 (1980).

[5] M. I. Holmes and T. Gustafsson, Phys. Rev. Lett. **47**, 443 (1981).

[6] W. Drube, D. Straub, F. J. Himpsel, P. Soukiassian, C. L. Fu, and A. J. Freeman, Phys. Rev. B **34**, 8989 (1986).

[7] K. S. Shin, H. W. Kim, and J. W. Chung, Surf. Sci. **385**, L978 (1997).

[8] D. Singh, Su-Huai Wei, and H. Krakauer, Phys. Rev. Lett. **57**, 3292 (1986).

[9] R. Yu, H. Krakauer, and D. Singh, Phys. Rev. B **45**, 8671 (1992).

[10] M. S. Altman, P. J. Estrup, and I. K. Robinson, Phys. Rev. B **38**, 5211 (1988).

[11] C. L. Fu and A. J. Freeman, Phys. Rev. B **37**, 2685 (1988).

[12] H. Ibach, Surf. Sci. Rep. **29**, 193 (1997).

[13] P. J. Berlowitz, J.-W. He, and D. W. Goodman, Surf. Sci. **231**, 315 (1990).

[14] H. J. Elmers and J. Hauschild, Surf. Sci. **320**, 134 (1994).

[15] G. A. Mulhollan, R. L. Fink, J. L. Erskine, and G. K. Walters, Phys. Rev. B **43**, 13 645 (1991).

[16] W. Wulfhekel, F. Zavaliche, R. Hertel, S. Bodea, G. Steierl, G. Liu, J. Kirschner, and H. P. Oepen, Phys. Rev. B **68**, 144416 (2003).

[17] U. Gradmann and G. Waller, Surf. Sci. **116**, 539 (1982).

[18] H. J. Elmers, G. Liu, and U. Gradmann, Phys. Rev. Lett. **63**, 566 (1989).

[19] M. Przybylski, I. Kaufmann, and U. Gradmann, Phys. Rev. B **40**, 8631 (1989).

[20] T.-U. Nahm and R. Gomer, Surf. Sci. **373**, 237 (1997).

[21] T.-U. Nahm and R. Gomer, Surf. Sci. **380**, 52 (1997).

[22] M. Albrecht, U. Gradman, Th. Reinert, and L. Fritsche, Solid State Commun. **70**, 671 (1991).

[23] E. D. Tober, R. X. Ynzunza, F. J. Palomares, Z. Wang, Z. Hussain, M. A. Van Hove, and C. S. Fadley, Phys. Rev. Lett. **79**, 2085 (1997).

[24] H. J. Elmers, J. Hauschild, H. Fritzsche, G. Liu, U. Gradmann, and U. Köhler, Phys. Rev. Lett. **75**, 2031 (1995).

[25] D. Sander, R. Skomski, C. Schmidthals, A. Enders, and J. Kirschner, Phys. Rev. Lett. **77**, 2566 (1996).

[26] H. Bethge, D. Heuer, Ch. Jensen, K. Reshöft, and U. Köhler, Surf. Sci. **331–333**, 878 (1995).

[27] R. Popescu, H. L. Meyerheim, D. Sander, J. Kirschner, S. Steadman, O. Robach, and S. Ferrer, Phys. Rev. B **68**, 155421 (2003).

[28] H. J. Elmers, J. Hauschild, and U. Gradmann, Phys. Rev. B **54**, 15 224 (1996).

[29] S. C. Hong, A. J. Freeman, and C. L. Fu, Phys. Rev. B **38**, 12 156 (1988).

[30] I. Galanakis, M. Alouani, and H. Dreyssé, Phys. Rev. B **62**, 3923 (2000).

[31] X. Qian and W. Hübner, Phys. Rev. B **60**, 16 192 (1999).

[32] X. Qian and W. Hübner, Phys. Rev. B **67**, 184414 (2003).

[33] J. Hauschild, H. J. Elmers, and U. Gradmann, Phys. Rev. B **57**, R677 (1998).

[34] H. J. Elmers, J. Hauschild, H. Höche, U. Gradmann, H. Bethge, D. Heuer, and U. Köhler, Phys. Rev. Lett. **73**, 898 (1994).

[35] H. J. Elmers, J. Hauschild, and U. Gradmann, J. Magn. Magn. Mater. **221**, 219 (2000).

[36] D. Reuter, G. Gerth, and J. Kirscher, Phys. Rev. B **57**, 2520 (1998).

[37] M. Arnold, L. Hammer, K. Heinz, B. Kohler, and M. Scheffler, Surf. Sci. **382**, 288 (1997).

[38] V. Fiorentini and M. Methfessel, J. Phys.: Condens. Matter **8**, 6525 (1996).

[39] H. L. Skriver and N. M. Rosengaard, Phys. Rev. B **46**, 7157 (1992).

[40] G. Kresse and J. Furthmüller, Phys. Rev. B **54**, 11 169 (1996); Comput. Mater. Sci. **6**, 15 (1996).

[41] P. Blöchl, Phys. Rev. B **50**, 17 953 (1994).

[42] G. Kresse and D. Joubert, Phys. Rev. B **59**, 1758 (1999).

[43] J. Perdew and A. Zunger, Phys. Rev. B **23**, 5048 (1981).

[44] J. P. Perdew, J. A. Chevary, S. H. Vosko, K. A. Jackson, M. R. Pedersen, D. J. Singh, and C. Fiolhais, Phys. Rev. B **46**, 6671 (1992).

[45] P. Villars and L. D. Calvert, *Pearson's Handbook of Crystallographic Data for Intermetallic Phases*, 2nd ed. (ASM International, Materials Park, Ohio, 1991).

[46] F. H. Featherston and J. R. Neighbours, Phys. Rev. **130**, 1324 (1963).

[47] H. J. Monkhorst and J. D. Pack, Phys. Rev. B **13**, 5188 (1976).

[48] G. Henkelman and H. Jónsson, J. Chem. Phys. **111**, 7010 (1999).

[49] C. M. Chang, C. M. Wei, and J. Hafner, J. Phys. Chem. **13**, L321 (2001).

[50] E. G. Moroni, G. Kresse, J. Hafner, and J. Furthmüller, Phys. Rev. B **56**, 15 629 (1997).

[51] G. L. Kellogg and P. J. Feibelman, Phys. Rev. Lett. **64**, 3143 (1990).

[52] G. L. Kellogg, Surf. Sci. Rep. **21**, 1 (1994).

[53] M. Pratzer, H. J. Elmers, and M. Getzlaff, Phys. Rev. B **67**, 153405 (2003).

[54] B. Lang, R. W. Joyner, and G. A. Somorjai, Surf. Sci. **30**, 454 (1972).